Numerical study on the hydrodynamic interactions between two ships arranged side by side

Zhi-Ming Yuan*, Atilla Incecik

Department of Naval Architecture, Ocean and Marine Engineering
University of Strathclyde, Glasgow, G4 0LZ, UK

Abstract: 3-D Rankine source method is used to investigate the hydrodynamic interactions between two ships arranged side by side with or without forward speed. A new radiation condition, which takes Doppler shift into account, is imposed on the control surface. The present method was validated through two pairs of models both in beam and head waves. Model 1 is about a modified Wigley hull and a rectangular box model at beam sea condition without speed and Model 2 is about a full scale supply ship and frigate model at head seam condition with forward speed. The method developed was validated through model experiments as well as the published numerical programs and a good agreement was obtained.
Keywords: Hydrodynamic interaction; Rankine source method; Radiation condition; Wave pattern; Forward speed.
Article ID: HS-SU-W

1 Introduction

Lightering operations with forward speed are important for the transfer of fuel in naval operations. Nowadays, lighting operations without forward speed is important for the LNG offloading from LNG FPSOs or FSRUs (Floating Storage and Regassification Units). The loads in the mooring lines between the two vessels, the loads in the floating fenders and the relative motions at the manifold location are the most critical issues during this operation. These are determined by the wave, wind and current loads on the two vessels in close proximity, as well as by the strong hydrodynamic interaction between the vessels. Even in head seas, the two vessels could be subjected to a very large separating force as the waves run between the two hulls. The resulting motions and mooring loads determine the operability of the operation in certain environmental conditions.

Early studies on the hydrodynamic interaction problem focused on 2-D strip theory. Ohkusu (1974) used the multipoles method and theory to calculate the response of parallel, slender, ship like bodies in beam waves. His results clearly illustrated the effect of position of a smaller body on the weather and lee side against a large body. Kodan (1984) extended Ohkusu's theory (Ohkusu, 1974) to hydrodynamic interaction between two parallel structures in oblique waves by strip method. Fang and Kim (1986) analysed the hydrodynamically coupled motions of two longitudinally parallel barges advancing in oblique waves by strip method. His analysis showed that the coupled motions of two advancing ships depend on the speed, wave heading and distance. The 2-D method was a simple and effective tool in predicting the hydrodynamic interaction between two adjacent ships. Ronæss (2002) applied a unified slender body theory to investigate the ship-to-ship with forward speed problem. Her results showed good agreement with her model tests at the Marine Technology Centre in Trondheim, Norway. However, the limitations of applying 2-D methods in the ship-to-ship interaction problem in waves have been confirmed by Fang and Kim (1986). The two ships were assumed to be in each other's near-field. The 2-D method overestimated the interaction effects due to the wave energy trapping between the two hulls in the frequency range which is important for ship motions, which also leads to the overestimation of the mean second-order wave loads on each ship. Besides, the strip theory can only predict the motion responses of conventional monohull ship in waves at low to moderate Froude numbers. However at high Froude numbers, three-dimensional (3-D) effects become dominant and strip theory fails to predict the hydrodynamic performance of vessels travelling with high forward speed. Under these circumstances, an advanced computational technique which accounts for the 3D flow interactions is necessary for motion and loading prediction.

Chen and Fang (2001) extended Fang's method (Fang and Kim, 1986) to 3-D. They used a 3-D Green function method to investigate the hydrodynamic problems between two moving ships in waves. It was found that the hydrodynamic interactions calculated by a 3-D method were more reasonable in the resonance region, where the responses were overestimated by 2-D method. However, their method was only validated by model tests with zero speed. More rigorous validation should be made by further experiments. Kim and Ha (2002) used 3-D pulsating source distribution techniques to calculate twelve coupled linear motion responses and

Received date: 28/04/2014
Foundation item: Supported by Lloyd's Register
***Corresponding author Email: zhiming.yuan@strath.ac.uk**

relative motions of the barge and the ship in oblique waves. Their computational results gave a good correlation with the experimental results and also with other numerical results. Taggart et al. (2003) and Li (2007) developed a frequency domain code based on 3-D Green function method. They validated their numerical predictions by model tests conducted at the Institute for Marine Dynamics (IMD) in St. John's, Newfoundland. It was showed that the presence of a larger ship could significantly influence the motions of a smaller ship in close proximity. But the numerical prediction of roll motion was not accurate. Xu and Faltinsen (2011) used a 3-D Rankine source method to solve the linear initial-boundary value problem of two ships advancing in waves. The time domain analysis was validated through the frequency solution via Fourier transform, and also the model test results. Recently, within the frame work of Green function, Xu and Dong (2013) developed a 3-D translating-pulsating (3DTP) source method to calculate wave loads and free motions of two ships advancing in waves. Model tests were carried out to measure the wave loads and the heave, roll and pitch motions for a pair of side-by-side arranged ship models advancing with an identical speed in head regular waves. Both the experiment and the numerical prediction showed that hydrodynamic interaction effects on wave loads and motions were significant. They also pointed out that the prediction accuracy of the 3DTP method was much better than that of 3DP, especially for peak values of the motion responses.

In the present study, the Rankine source approach proposed by Hess and Smith (Hess and Smith, 1964) will be applied, which uses a very simple Green function in the boundary integral formulation. This method requires the sources distributed not only on the body surface, but also on the free surface, control surface and sea bottom. Therefore, a flexible choice of free-surface condition and sea bottom condition can be realized in these methods. The forward speed can be directly taken into the consideration in the boundary value problem. Besides, the near field wave elevations can be directly obtained by boundary integration on the free surface. In order to complete the boundary value problem, a radiation condition should be imposed on the control surface. A commonly used treatment was proposed by Nakos (1990). The free surface was truncated at some upstream points, and two boundary conditions were imposed at these points to ensure the consistency of the upstream truncation of the free surface. Another method to deal with the radiation condition is to move the source points on the free surface at some distance downstream (Jensen et al., 1986). The results from these two methods show very good agreement with published experimental data when the Brard number τ ($\tau = u\omega/g$) is greater than 0.25, since they are both based on the assumption that there is no scattered wave travelling ahead of the vessel. However, when the forward speed of the vessel is very low, the Brard number will be smaller than 0.25 and the scattered waves could travel ahead of the vessel. These traditional radiation conditions could no longer be valid. For ship-to-ship problem, the forward speed is usually limited to a low level for the safe operations. Therefore, a new extensive radiation condition is required to deal with the very low forward speed problem. Das and Cheung (2012a, b) provided an alternate solution to the boundary-value problem for forward speeds above and below the group velocity of the scattered waves. They corrected the Sommerfeld radiation condition by taking into account the Doppler shift of the scattered waves at the control surface that truncates the infinite fluid domain. They compared their results with the experimental data, and good agreement was achieved. They also computed the wave elevation on the free surface, and a reasonable wave pattern was obtained at $\tau<0.25$ by using their new radiation condition. In this paper, we will extend Das and Cheung's radiation condition to the ship-to-ship problem. A 3-D panel code based on Rankine source method will be developed to investigate the hydrodynamic interaction between two vessels arranged side by side with forward speed. The motion responses of both ships will be calculated and compared to these obtained from commercial software and experimental results.

2 Formulations of the potentials

2.1 Coordinate systems

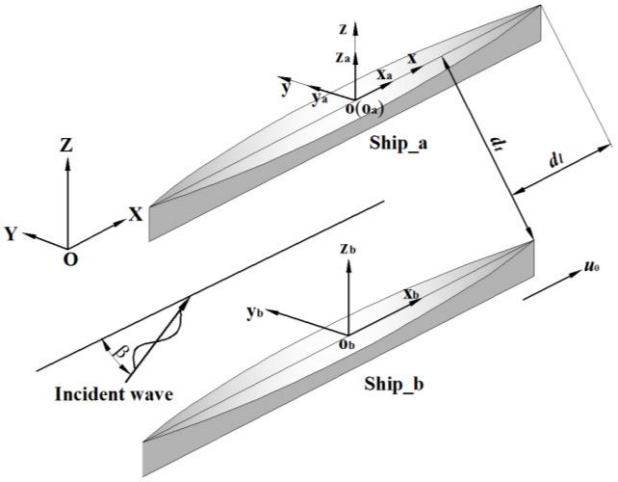

Fig. 1 An example vessels and coordinate system

The corresponding right-handed coordinate systems are shown in Fig. 1 (Yuan and Incecik). The body coordinate systems o_a-$x_a y_a z_a$ and o_b-$x_b y_b z_b$ are fixed on ship_a and ship_b respectively with their origins on the mean free surface, coinciding with the corresponding centre of gravity (CoG) in respect to x and y coordinates when both of the ships are at their static equilibrium positions. o_a-z_a and o_b-z_b are both positive upward. The inertia coordinate system o-xyz with origin located on the calm free surface coincides with o_a-$x_a y_a z_a$ when the ship has no unsteady motions. *O-XYZ* is the earth-fixed coordinate system with its origin located on the calm free surface and *OZ* axis positive upward. Three components of translation motions include surge (η_1^a and η_1^b , which are parallel to x-axis), sway (η_2^a

and η_2^b, which are parallel to y-axis) and heave (η_3^a and η_3^b, which are parallel to z-axis). Another three rotational motion components are roll (η_4^a and η_4^b, which rotate around x-axis), pitch (η_5^a and η_5^b, which rotate around y-axis) and yaw (η_6^a and η_6^b, which rotate around z-axis). The incident wave direction is defined as the angle between the wave propagation direction and X-axis. β=180° corresponds to head sea; β=90° corresponds to beam sea. *dt* denotes the transverse distance between two ships while *dl* is the longitudinal distance. u_0 is the forward speed.

In the computation, the motions and forces of ship-a and ship-b are concerted to the local coordinate system in which the origin is at the center of gravity of each ship.

2.2 Diffraction and radiation potential

It is assumed that the surrounding fluid is inviscid and incompressible, and that the motion is irrotational, the total velocity potential exists which satisfies the Laplace equation in the whole fluid domain. Let t denote time and $\vec{\mathbf{x}}=(x,y,z)$ the position vector. A complex velocity potential provides a description of the flow as

$$\psi(\vec{\mathbf{x}},t)=u_0\left[\varphi_s(\vec{\mathbf{x}})-x\right]+\mathrm{Re}\sum_{j=1}^{6}[\eta_j^a\varphi_j^a(\vec{\mathbf{x}})e^{-i\omega_e t}+\eta_j^b\varphi_j^b(\vec{\mathbf{x}})e^{-i\omega_e t}]$$
$$+\mathrm{Re}[\eta_0\varphi_0(\vec{\mathbf{x}})e^{-i\omega_e t}]+\mathrm{Re}[\eta_7\varphi_7(\vec{\mathbf{x}})e^{-i\omega_e t}],\ j=1,2,...,6 \tag{1}$$

where φ_s is the steady potential and it is neglected in the present study; φ_j^a and φ_j^b (j=1,2,…,6) are the spatial radiation potential in six degrees of freedom corresponding to the oscillations of Ship_a and Ship_b respectively and η_j *(j=1,2,…6)* is the corresponding motion amplitude (η_1, surge; η_2, sway; η_3, heave; η_4, roll; η_5, pitch; η_6, yaw); $\eta_7=\eta_0$ is the incident wave amplitude; φ_7 is the spatial diffraction potential; φ_0 is the spatial incident wave potential and ω_e is the encounter frequency. Generally, the body boundary conditions can be treated separately by the diffraction and radiation problem as follows:

1) Body boundary conditions for the diffraction problem:

$$\frac{\partial\varphi_7}{\partial n}=-\frac{\partial\varphi_0}{\partial n}\Big|_{S_a} \tag{2}$$

$$\frac{\partial\varphi_7}{\partial n}=-\frac{\partial\varphi_0}{\partial n}\Big|_{S_b} \tag{3}$$

2) Body boundary conditions for the radiation problem (Ship_a is oscillating while Ship_b is fixed):

$$\frac{\partial\varphi_j^a}{\partial n}=-i\omega_e n_j^a+u_0 m_j^a\Big|_{S_a} \tag{4}$$

$$\frac{\partial\varphi_j^a}{\partial n}=0\Big|_{S_b} \tag{5}$$

3) Body boundary conditions for the radiation problem (Ship_b is oscillating while Ship_a is fixed):

$$\frac{\partial\varphi_j^b}{\partial n}=-i\omega_e n_j^b+u_0 m_j^b\Big|_{S_b} \tag{6}$$

$$\frac{\partial\varphi_j^b}{\partial n}=0\Big|_{S_a} \tag{7}$$

where $\vec{n}=(n_1,n_2,n_3)$ is the unit normal vector directed inward on body surface, $\vec{x}=(x,y,z)$ is the position vector on body surface. The m_j denotes the *j*-th component of the so-called *m*-term,

$$\begin{aligned}(m_1,m_2,m_3)&=(0,0,0)\\(m_4,m_5,m_6)&=(0,n_3,-n_2)\end{aligned} \tag{8}$$

The free surface boundary for both diffraction and radiation problem can be written as:

$$g\frac{\partial\varphi_j}{\partial z}-\omega_e^2\varphi_j+2i\omega_e u_0\frac{\partial\varphi_j}{\partial x}+u_0^2\frac{\partial^2\varphi_j}{\partial x^2}=0,\quad j=1,2,...7 \tag{9}$$

The radiation condition ensures that the waves propagate away from the ship. **Fig. 2** illustrates the Doppler shift of the scattered wave field of single ship advancing in the positive x direction and its effect on the implementation of the radiation condition.

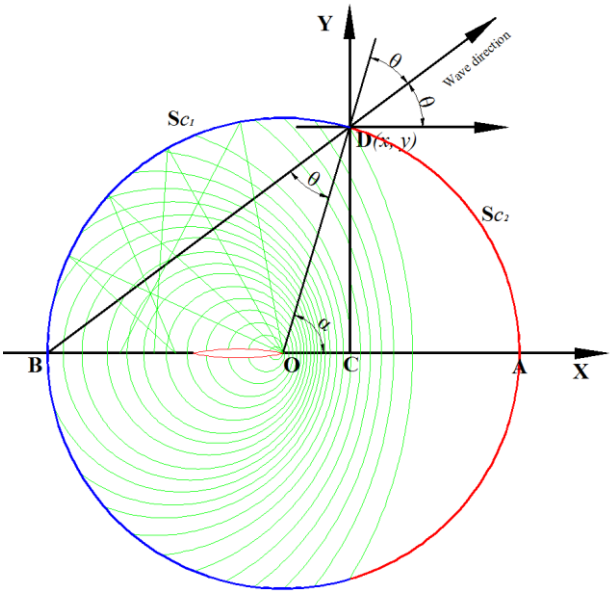

Fig. 2 Sketch of Doppler shift and radiation condition of single ship

When the vessel speed exceeds the group velocity of the scattered waves, a quiescent region emerges ahead. The waves reaching point D have their wave direction rotated by an angle θ relative to the radial axis and their apparent origin shifted downstream to point B. The scattered waves at a large distance from the vessel behave similar to those from a point source, giving rise to the kinematic condition

$BO/u_0=BD/c$, where c is the velocity of the scattered waves in absence of the current. This relation determines the local wave number k_s and rotated angle θ at any points on the control surface. The radiation condition then can be written as

$$\frac{\partial \varphi_j}{\partial n} - ik_s \varphi_j \cos\theta = 0 \quad (j=1, 2, \dots, 6) \quad \text{on } S_{c1} \tag{10}$$

$$\nabla \varphi_j = 0 \quad (j=1, 2, \dots, 6) \quad \text{on } S_{c2} \tag{11}$$

where S_{c1} and S_{c2} denote the portions of control surface with and without scattered waves (Das and Cheung, 2012b).

3 Equation of motion

Once the unknown diffraction potential φ_7 and radiation potential φ_j (j=1,2,…6) are solved, the time-harmonic pressure can be obtained from Bernoulli's equation:

$$p_j = -\rho\left[i\omega_e \eta_j \varphi_j + \nabla(\varphi_s - u_0 x)\cdot\nabla \eta_j \varphi_j \right], j=0, 1, \dots, 7 \tag{12}$$

where ρ is the fluid density. The hydrodynamic force produced by the oscillatory motions of the vessel in the six degrees of freedom can be derived from the radiation potentials as

$$F_i^{Ra} = \sum_{j=1}^{6} \iint_{S_a} p_j^a n_i dS \cdot (\eta_j^a + \eta_j^b)$$

$$= \sum_{j=1}^{6} \left[\omega_e^2 \mu_{ij}^{aa} + i\omega \lambda_{ij}^{aa} \right] \eta_j^a + \sum_{j=1}^{6} \left[\omega_e^2 \mu_{ij}^{ab} + i\omega \lambda_{ij}^{ab} \right] \eta_j^b \quad i=1, 2, \dots, 6 \tag{13}$$

$$F_i^{Rb} = \sum_{j=1}^{6} \iint_{S_b} p_j^b n_i dS \cdot (\eta_j^a + \eta_j^b)$$

$$= \sum_{j=1}^{6} \left[\omega_e^2 \mu_{ij}^{ba} + i\omega_e \lambda_{ij}^{ba} \right] \eta_j^a + \sum_{j=1}^{6} \left[\omega_e^2 \mu_{ij}^{bb} + i\omega_e \lambda_{ij}^{bb} \right] \eta_j^b \quad i=1, 2, \dots, 6 \tag{14}$$

The added mass and damping can be expressed respectively as:

$$\begin{aligned}
\mu_{ij}^{aa} &= -\frac{\rho}{\omega_e} \iint_{S_a} (\varphi_{Ij}^a - \frac{u_0}{\omega_e} \frac{\partial \varphi_{Rj}^a}{\partial x}) n_i ds \\
\mu_{ij}^{ab} &= -\frac{\rho}{\omega_e} \iint_{S_a} (\varphi_{Ij}^b - \frac{u_0}{\omega_e} \frac{\partial \varphi_{Rj}^b}{\partial x}) n_i ds \\
\mu_{ij}^{bb} &= -\frac{\rho}{\omega_e} \iint_{S_b} (\varphi_{Ij}^b - \frac{u_0}{\omega_e} \frac{\partial \varphi_{Rj}^b}{\partial x}) n_i ds \\
\mu_{ij}^{ba} &= -\frac{\rho}{\omega_e} \iint_{S_b} (\varphi_{Ij}^a - \frac{u_0}{\omega_e} \frac{\partial \varphi_{Rj}^a}{\partial x}) n_i ds \\
&(i=1, 2, \dots, 6; j=1, 2, \dots, 6)
\end{aligned} \tag{15}$$

$$\begin{aligned}
\lambda_{ij}^{aa} &= -\rho \iint_{S_a} (\varphi_{Rj}^a + \frac{u_0}{\omega_e} \frac{\partial \varphi_{Ij}^a}{\partial x}) n_i ds \\
\lambda_{ij}^{ab} &= -\rho \iint_{S_a} (\varphi_{Rj}^b + \frac{u_0}{\omega_e} \frac{\partial \varphi_{Ij}^b}{\partial x}) n_i ds \\
\lambda_{ij}^{bb} &= -\rho \iint_{S_b} (\varphi_{Rj}^b + \frac{u_0}{\omega_e} \frac{\partial \varphi_{Ij}^b}{\partial x}) n_i ds \\
\lambda_{ij}^{ba} &= -\rho \iint_{S_b} (\varphi_{Rj}^a + \frac{u_0}{\omega_e} \frac{\partial \varphi_{Ij}^a}{\partial x}) n_i ds \\
&(i=1, 2, \dots, 6; j=1, 2, \dots, 6)
\end{aligned} \tag{16}$$

where μ_{ij}^{aa} is the added mass of Ship_a in i-th mode which is induced by the motion of Ship_a in j-*th* mode; μ_{ij}^{ab} is the added mass of Ship_a in i-th mode which is induced by the motion of Ship_b in j-th mode; μ_{ij}^{ba} is the added mass of Ship_b in i-th mode which is induced by the motion of Ship_a in j-th mode; μ_{ij}^{bb} is the added mass of Ship_b in i-th mode which is induced by the motion of Ship_b in j-th mode; λ is the added damping and the definition the subscript is the same as that of added mass; φ_{Rj} is the real part of j-*th* potential, and φ_{Ij} is the imaginary part. The wave excitation force can be obtained by the integration of incident and diffraction pressure as

$$F_i^{Wa} = \iint_{S_a} (p_0 + p_7) n_i dS \tag{17}$$

$$F_i^{Wb} = \iint_{S_b} (p_0 + p_7) n_i dS \tag{18}$$

Applying Newton's second law, the 12 components of ship motions in the frequency domain can be obtained by solving the following equation system:

$$\begin{aligned}
&\sum_{j=1}^{6} \left\{ \left[-\omega_e^2 \left(M_{ij}^a + \mu_{ij}^{aa} \right) + i\omega_e \lambda_{ij}^{aa} + K_{ij}^a \right] \eta_j^a \right. \\
&\left. + \left[-\omega_e^2 \mu_{ij}^{ab} + i\omega_e \lambda_{ij}^{ab} \right] \eta_j^b \right\} = F_i^{Wa} \\
&\quad i=1, 2, \dots, 6
\end{aligned} \tag{19}$$

$$\begin{aligned}
&\sum_{j=1}^{6} \left\{ \left[-\omega_e^2 \mu_{ij}^{ba} + i\omega_e \lambda_{ij}^{ba} \right] \eta_j^a \right. \\
&\left. + \left[-\omega_e^2 \left(M_{ij}^b + \mu_{ij}^{bb} \right) + i\omega_e \lambda_{ij}^{bb} + K_{ij}^b \right] \eta_j^b \right\} = F_i^{Wb} \\
&\quad i=1, 2, \dots, 6
\end{aligned} \tag{20}$$

where M_{ij}^a and M_{ij}^b represent the generalized mass matrix for Ship_a and Ship_b; K_{ij}^a and K_{ij}^b represent the restoring matrix for Ship_a and Ship_b.

4 Validations and discussion

In this section, we will validate our program through a numerical study about two ships stationary or travelling in waves. The validation is established through two pairs of models. Model 1 is about a modified Wigley hull and a box model at beam sea case and the experimental results as well as some published results will be used for the validation. Model 2 is about a full scale supply ship and frigate model at head seam condition with forward speed and the model test results, as well as the published numerical results, will be used for the comparison.

4.1 Validations of two ships stationary in beam waves

Model 1 is about a modified Wigley hull (Ship_a) and a rectangular box (Ship_b) model at beam sea condition. The modified model can be defined as (Kashiwagi et al., 2005)

$$\frac{2y}{B}=\left[1-\left(\frac{2x}{L}\right)^2\right]\left[1-\left(\frac{z}{T}\right)^2\right]\left[1+0.2\left(\frac{2x}{L}\right)^2\right]+\left(\frac{z}{T}\right)^2\left[1-\left(\frac{z}{T}\right)^8\right]\left[1-\left(\frac{2x}{L}\right)^2\right]^4 \quad (21)$$

where B is the breadth, L is the length and T is the draft of the ship. The main dimensions of the modified Wigley and the rectangular box are shown in Table 1.

Table 1
Main dimensions of the modified Wigley hull and the box (Kashiwagi et al., 2005)

	Modified Wigley hull	Rectangular box
Length between perpendicular	L_a=2 *m*	L_b=2 *m*
Breadth	B_a=0.3 *m*	B_b=0.3 *m*
Draught	T_a=0.125 *m*	T_b=0.125 *m*
Displacement	V_a=0.04205 *t*	V_b=0.0375 *t*
Water-plane area	A_{wa}=0.416 m^2	A_{wb} =0.60 m^2

Two typical cases are simulated here:

1) Ship_a is situated in the weather side and Ship_b is in the lee side. The transverse (*dt*) and longitudinal distance (*dl*) between the two ships is 1.097 *m* and 0 *m* respectively.
2) Ship_a is situated in the lee side and Ship_b is in the weather side. The transverse (*dt*) and longitudinal distance (*dl*) between the two ships is 1.797 *m* and 0 *m* respectively.

The computational range on the free surface is extended to 2*L* upstream, 2*L* downstream and 2*L* sideways, where *L*=2 *m* is the length of the vessel. For the case of *dt*=1.079, there are 320 panels on the body surface of Wigley hull, 480 on the body surface of the rectangular box, 7800 on free surface and 2052 on the control surface, which is shown in **Fig. 3**. For the case of *dt*=1.797, there are 320 panels on the body surface of Wigley hull, 480 on the body surface of the rectangular box, 8360 on free surface and 1780 on the control surface.

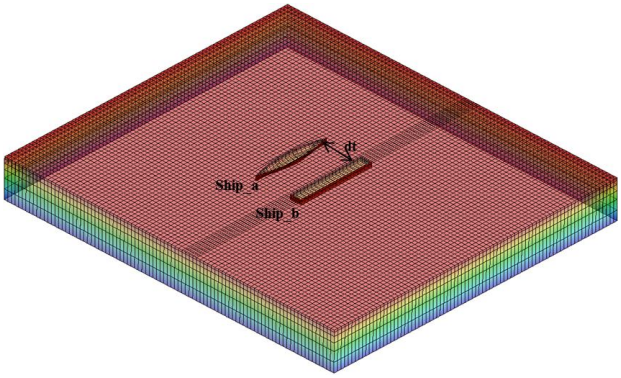

Fig. 3 Computational domain and panel distribution of a modified Wigley hull and a rectangular box model stationary in waves at *dt*=1.079.

Fig. 4 shows the hydrodynamic coefficients of a modified Wigley hull due to the heave motion of the Wigley hull itself when the rectangular box is fixed with the separation distance of *dt*=1.797 *m*, where $K=\omega_0^2 L_c/g$ and L_c is the characteristic length scale for nondimension (which is taken as $L_c = L_a/2$). The comparisons with experimental data and Green function method (Kashiwagi et al., 2005) are also included. The numerical results calculated by the present 3-D Rankine source method generally agree with the experimental data. The hydrodynamic interactions are properly accounted for, especially for the sway added mass and damping (μ_{23}^{aa} and λ_{23}^{aa}) which are exerted only by wave interactions between Ship_a and Ship_b. Some discrepancies can be observed in the heave added mass and damping (μ_{33}^{aa} and λ_{33}^{aa}) at low frequency range, which may be attributed to the effect of the reflection waves from the parallel side walls of the tank, as explained by Kashiwagi et al. (2005).

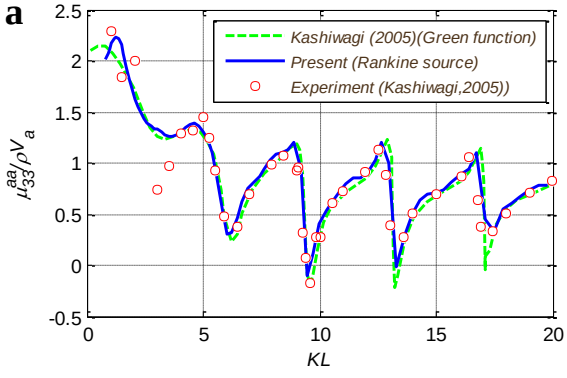

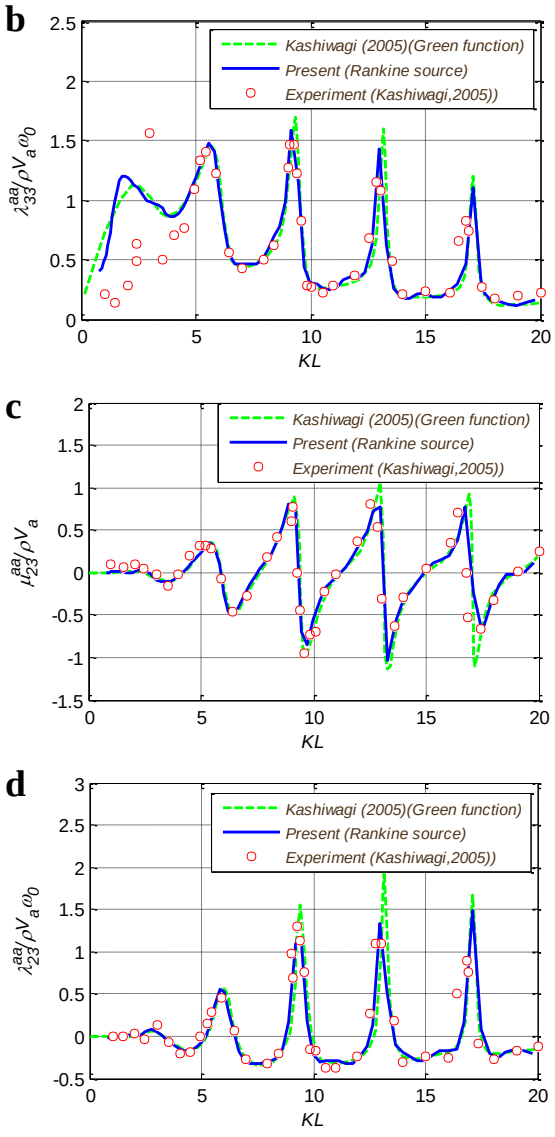

Fig. 4 Hydrodynamic coefficients of a modified Wigley hull due to the heave motion of the Wigley hull itself when the rectangular box is fixed with the separation distance of dt=1.797 m. (a) Heave added mass; (b) Heave damping; (c) Sway added mass; (d) Sway damping.

Fig. 5 shows the wave excitation forces on the modified Wigley hull (Ship_a, in the weather side) and rectangular box (Ship_b, in the lee side) with the separation distance of dt=1.097 m. The overall agreement between measured and computed results is good, although slight discrepancies can be seen in a range of long wavelengths, which is due to the reflection wave effects from the side walls of the tanker. Very good agreement has been obtained between the present Rankine source method and Green function method. It can be concluded that both Green function method and Rankine source method can predict the hydrodynamic forces of two ships arranged side by side with zero speed in beam waves.

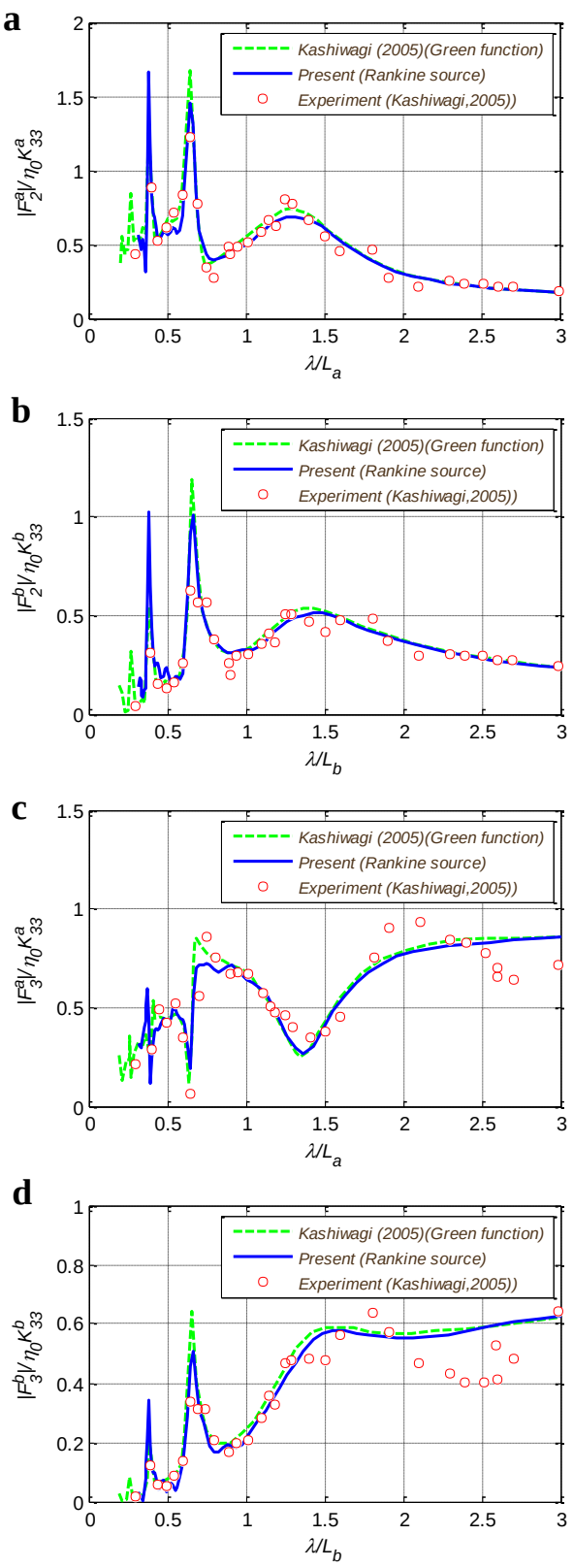

Fig. 5 Wave excitation forces in beam waves with the transverse distance between two ships of dt=1.097 m. (a) Sway forces on Ship_a; (b) Sway forces on Ship_b; (c) Heave forces on Ship_a; (d) Heave forces on Ship_b;

4.1 Validations of two ships travelling in head waves

The main particulars of supply ship (Ship_a) and frigate (Ship_b) are shown in **Table 2**. The transverse and longitudinal distances between two ships are 52.702 m and 0 m respectively. A typical case is simulated here: head sea with forward speed of 6.18 m/s. To be consistent with the model tests condition, both ships are restrained in surge, sway and yaw while the motions in heave, roll and pitch are free. In order to make comparison, we also present the numerical results of two ships at zero forward speed. The computational domain is shown in **Fig. 6**. The free surface is truncated at L_a upstream, $2L_a$ downstream, L_a in the supply ship sideward and L_b in the frigate sideward. There are 378 panels on the body surface of supply ship, 5400 on free surface, 2432 on the control surface and 414 on the body surface of frigate.

Table 2
Main particulars of supply ship and frigate (Li, 2001)

	Supply ship	Frigate
Length between perpendicular	L_a=180 m	L_b=122 m
Breadth	B_a=30.633 m	B_b=14.78 m
Draught	T_a=8.5 m	T_b=4.5 m
Displacement	V_a=28223.3 t	V_b=4023.7 t
Block coefficient	C_B^a =0.588	C_B^b =0.484
Longitudinal CoG (rel. midship)	X_G^a =-1.688 m	X_G^b =3.284 m
Vertical CoG (rel. calm waterline)	Z_G^a =3.925 m	Z_G^b =2.049 m
Radius of inertia for roll	r_{44}^a =8.047 m	r_{44}^b =4.921 m
Radius of inertia for pitch	r_{55}^a =45 m	r_{55}^b =30.5 m
Radius of inertia for yaw	r_{66}^a =45 m	r_{66}^b =30.5 m

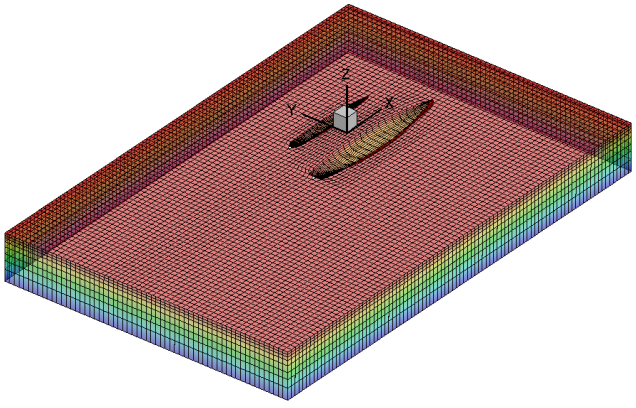

Fig. 6 Computational domain of Model 1

Fig. 7 shows the response amplitudes of two ships in heave, roll and pitch motions. The comparisons with experimental data and Green function method (Li, 2007) are also included. The numerical results calculated by the present 3-D Rankine source method generally agree with the experimental data. In order to investigate the speed effect, we also present the results of two ships without forward speed. It can be observed that the increase of the response amplitude operators with forward speed is considerable, especially for the smaller ship (Ship_b). Roll motion of Ship_a is obviously reduced due to the forward speed. But for Ship_b, the roll motion increases dramatically at $\lambda/L>1$ due to the forward speed. We also find the roll motions of both ships are significantly influenced by the roll damping coefficient. It is found that the damping in roll cannot be predicted well by the radiation component only (Chakrabarti, 2001). The difficulty in predicting the roll motion arises from the nonlinear characteristics of roll due to the effect of fluid viscosity. In ship-to-ship problem, the roll motion is always remarkable due to the hydrodynamic interaction between two ships. The present potential flow theory is based on the assumption that the surrounding fluid is inviscid and it cannot predict the roll damping precisely. To complement the viscid component, an equivalent linear damping coefficient is applied in the present study. The non-dimensional roll damping coefficient, κ , is given by

$$\kappa = \frac{\lambda_{44} + \lambda_{44v}}{2 \cdot \sqrt{(I_{44} + \mu_{44}) \cdot K_{44}}} \tag{22}$$

where λ_{44v} is the viscous damping. This damping coefficient is written as a fraction between the actual damping coefficient, $\lambda_{44} + \lambda_{44v}$, and the critical damping coefficient, $2 \cdot \sqrt{(I_{44} + \mu_{44}) \cdot K_{44}}$. **Fig. 8** is the numerical results of roll motion amplitudes of two ships at different damping coefficients. We find that κ_a=0.2 and κ_b=0.6 agree with the experimental results better than other values. This is because the roll motion of Ship_a is relatively small, while the roll motion of Ship_b is extremely large. Correspondingly, the nonlinear viscous characteristics of roll motion of Ship_b are more obvious. A larger equivalent linear damping coefficient should be used in the numerical simulations.

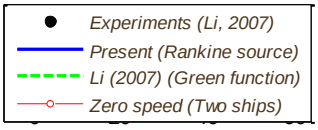

a

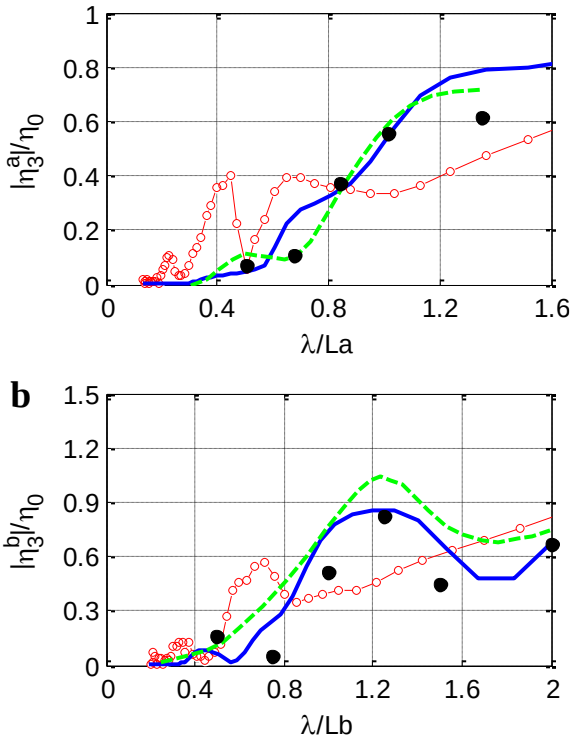

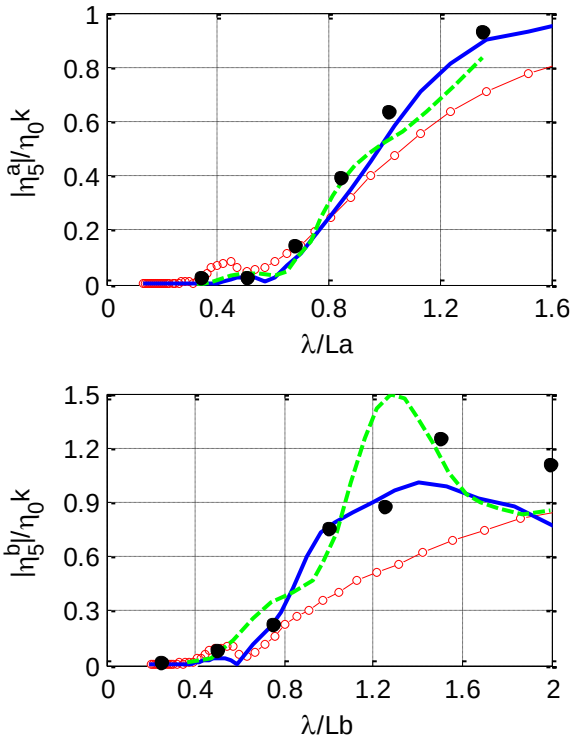

Fig. 7 Response amplitude operators. (a) Heave of ship_a; (b) Heave of Ship_b; (c) Roll of ship_a; (d) Roll of Ship_b; (e) Pitch of ship_a; (f) Pitch of Ship_b.

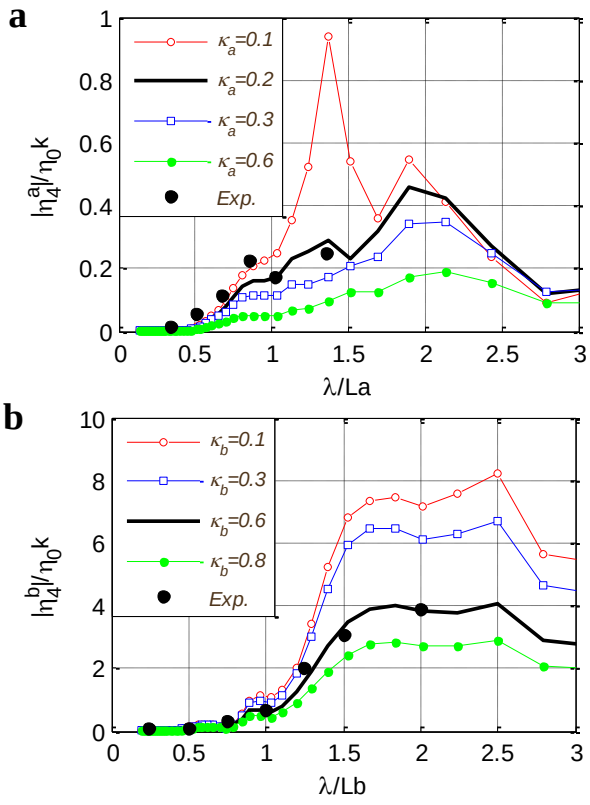

Fig. 8 Roll motion amplitudes at different damping coefficients. (a) Ship_a; (b) Ship_b.

5 Conclusions

In this paper, a boundary element program based on 3-D Rankine source method was developed to investigate the ship-to-ship interaction with or without forward speed problem. The radiation condition is satisfied by a modified Sommerfield radiation condition that takes Doppler shift into account while the Rankine-type Green function can satisfy the seabed boundary condition through the method of image. In order to eliminate the singularity on the free surface, we raise the source point at a short distance above the calm water level.

We validate the present program through two pairs of models in head seas. Model 1 is about a modified Wigley hull and a box model at beam sea case and the experimental results as well as some published results were used for the validation. Model 2 is about a full scale supply ship and frigate model at head seam condition with forward speed and the model test results, as well as the published numerical results, were used for the comparison. Good agreement has been achieved. The present method turns to be more time-consuming due to the modelling and solving the huge full rank matrix. However, the advantage of the present method lies on the two ships travelling with forward speed in the restricted waters, which was validated in Model 2. We compare the present calculation with the experimental data and find that the present prediction of heave and pitch motions has a satisfied agreement with the published experimental data. However, the prediction of roll motion is full of challenges due to the inviscid assumption in the potential flow theory, as well as the model test set-up.

Acknowledgement

The present work is mainly funded by Lloyd's Register. Authors are grateful to Lloyd's Register for their support.

References

Chakrabarti, S., 2001. Empirical calculation of roll damping for ships and barges. *Ocean Engineering* 28, 915-932.

Chen, G.R., Fang, M.C., 2001. Hydrodynamic interactions between two ships advancing in waves. *Ocean Engineering* 28, 1053-1078.

Das, S., Cheung, K.F., 2012a. Hydroelasticity of marine vessels advancing in a seaway. *Journal of Fluids and Structures* 34, 271-290.

Das, S., Cheung, K.F., 2012b. Scattered waves and motions of marine vessels advancing in a seaway. *Wave Motion* 49 (1), 181-197.

Fang, M.C., Kim, C.H., 1986. Hydrodynamically coupled motions of two ships advancing in oblique waves. *Journal of Ship Reaearch* 30 (3), 159-171.

Hess, J.L., Smith, A.M.O., 1964. Calculation of nonlifting potential flow about arbitrary three-dimensional bodies. *Journal of Ship Reaearch* 8 (2), 22-44.

Jensen, G., Mi, Z.X., Söding, H., 1986. Rankine source methods for numerical solutions of steady wave resistance problem, *Proceedings of 16th Symposium on Naval Hydrodynamics*, Berkeley, pp. 575-582.

Kashiwagi, M., Endo, K., Yamaguchi, H., 2005. Wave drift forces and moments on two ships arranged side by side in waves. *Ocean Engineering* 32 (5-6), 529-555.

Kim, M.S., Ha, M.K., 2002. Prediction of motion responses between two offshore floating structures in waves. *Journal of Ship & Ocean Technology* 6 (3), 13-25.

Kodan, N., 1984. The motions of adjacent floating structures in oblique waves, *Proceedings of the 3rd International Conference on Offshore Mechanics and Arctic Engineering*, New Orleans, pp. 206-213.

Li, L., 2001. Numerical seakeeping predictions of shallow water effect on two ship interactions in waves, PhD Thesis. Dalhousie University.

Li, L., 2007. Numerical seakeeping simulation of model test condition for two-ship interaction in waves, *Proceedings of the 26th International Conference on Offshore Mechanics and Arctic Engineering*, San Diego, California, USA, pp. OMAE2007-29328.

McTaggart, K., Cumming, D., Hsiung, C.C., Li, L., 2003. Seakeeping of two ships in close proximity. *Ocean Engineering* 30 (8), 1051-1063.

Nakos, D.E., 1990. Ship wave patterns and motions by a three dimensional Rankine panel method, PhD Thesis. MIT.

Ohkusu, M., 1974. Ship motions in vicinity of a structure, *Proceeding of International Conference on Behaviour of Offshore Structure*, NIT,Trondheim, pp. 284-306.

Ronæss, M., 2002. Wave induced motions of two ships advancing on parallel course, PhD Thesis. NTNU.

Xu, X., Faltinsen, O.M., 2011. Time domain simulation of two interacting ships advancing parallel in waves, *Proceedings of the 30th International Conference on Offshore Mechanics and Arctic Engineering*, Rotterdam, The Netherlands, pp. OMAE2011-49484.

Xu, Y., Dong, W.C., 2013. Numerical study on wave loads and motions of two ships advancing in waves by using three-dimensional translating-pulsating source. *Acta Mechanica Sinica* 29 (4), 494-502.

Yuan, Z.M., Incecik, A., Validation of a new radiation condition for two ships advancing in waves. Submit to *Journal of Fluid Mechanics*.